Microsc. Microanal. 19, 79–84, 2013
doi:10.1017/S1431927612013876

Microscopy AND Microanalysis

© MICROSCOPY SOCIETY OF AMERICA 2013

FIB Preparation of a NiO Wedge-Lamella and STEM X-Ray Microanalysis for the Determination of the Experimental k(O-Ni) Cliff-Lorimer Coefficient

Aldo Armigliato,[1,*] Stefano Frabboni,[2,3] Gian Carlo Gazzadi,[3] and Rodolfo Rosa[4]

[1]*CNR-IMM Institute, Via P.Gobetti, 101 40129 Bologna, Italy*
[2]*Dipartimento di Fisica, Università di Modena e Reggio Emilia, Via G. Campi 213/A, 41100 Modena (Italy) and CNR-Istituto di Nanoscienze-S3, via G. Campi 213/A, 41100 Modena, Italy*
[3]*CNR-Istituto di Nanoscienze-S3, via G. Campi 213/a, 41100 Modena, Italy*
[4]*Dipartimento di Scienze Statistiche, Università di Bologna, Via Belle Arti, 40126 Bologna, Italy*

Abstract: A method for the fabrication of a wedge-shaped thin NiO lamella by focused ion beam is reported. The starting sample is an oxidized bulk single crystalline, ⟨100⟩ oriented, Ni commercial standard. The lamella is employed for the determination, by analytical electron microscopy at 200 kV of the *experimental* k(O-Ni) Cliff-Lorimer (G. Cliff & G.W. Lorimer, *J Microsc* **103**, 203–207, 1975) coefficient, according to the extrapolation method by Van Cappellen (E. Van Cappellen, *Microsc Microstruct Microanal* **1**, 1–22, 1990). The result thus obtained is compared to the *theoretical* k(O-Ni) values either implemented into the commercial software for X-ray microanalysis quantification of the scanning transmission electron microscopy/energy dispersive spectrometry equipment or calculated by the Monte Carlo method. Significant differences among the three values are found. This confirms that for a reliable quantification of binary alloys containing light elements, the choice of the Cliff-Lorimer coefficients is crucial and experimental values are recommended.

Key words: FIB lamella, analytical electron microscopy, nickel-oxide films, Cliff-Lorimer factor, extrapolation method, Monte Carlo simulation

Introduction

Quantitative thin film X-ray microanalysis in the transmission electron microscope (TEM) is often performed by using the so-called Cliff-Lorimer approach (Cliff & Lorimer, 1975), which relates the concentration ratio $C(A)/C(B)$ in a binary alloy AB to the local X-ray intensity ratio $I(A)/I(B)$, through a coefficient k(A-B). In most commercial software packages implemented into the energy dispersive spectrometers, employing this *standardless* analysis method, the k(A-B) are generally *calculated*, assuming specific values for the ionization cross section Q, the fluorescence yield ω, the weight of the line a, and the detector efficiency ε. While for binary alloys consisting of medium and high atomic number elements this is acceptable, for alloys containing light elements such as the Ni-O film investigated in this article, the coefficients may be inaccurate (Cliff & Lorimer, 1975; Westwood et al., 1992; Williams & Carter, 2009); this problem was also found by us in the quantitative X-ray microanalysis of a commercial NiO/C thin film (Egerton & Cheng, 1994) when using a calculated k(O-Ni) factor. Therefore, for quantification purposes *experimental* k(O-Ni) coefficients are recommended. To obtain this, not only must suitable Ni-O standards be available, but the knowledge of the local thickness is also required.

This latter limitation is not tolerated by the extrapolation method, reported by Van Cappellen (1990), which is based on the extrapolation to zero of a plot $C(A)/C(B)$ versus X-ray intensity peaks ($I(A)$ or $I(A) + I(B)$), obtained from spectra taken in a series of points of the sample at different thicknesses. This (*virtual*) concentration ratio is deduced from a quantification obtained by imposing that the k coefficients are equal to 1; dividing it by the *true* composition of the binary standard AB yields the experimental k(A-B) coefficient.

The aim of this work is, first, the description of a focused ion beam (FIB)-based procedure to prepare a wedge-shaped thin lamella in a controlled way, starting from a surface-oxidized bulk Ni standard. Second, to perform quantitative X-ray microanalysis in points of increasing thickness of the wedge-shaped lamella in a scanning TEM (STEM) at 200 kV, thus obtaining, by the extrapolation method, the *experimental* k(O-Ni) coefficient. For comparison, the corresponding *theoretical* k values, obtained by both the Monte Carlo method and a commercial software for thin film EDS microanalysis, are also reported.

Experimental Techniques

Preparation of the NiO/Ni Standard

To realize a NiO film suitable for application as a standard in STEM X-ray microanalysis, we started from a commercial bulk, ⟨100⟩ oriented, Ni cylindrical sample (Goodfellow Cambridge Ltd., Huntington, UK, www.goodfellow.com), 12 mm in diameter and 2 mm thick. Its purity is guaranteed to be better than 99%. First, the standard has been polished by a lapping step with grits, followed by a treatment with an alumina paste, then annealed in a furnace for 1 h at 900°C in an atmosphere of slight Ar overpression to remove any

Received April 3, 2012; accepted August 19, 2012
**Corresponding author*: E-mail: armigliato@bo.imm.cnr.it

surfacial oxide. Then it has been subjected to a thermal treatment in a different furnace for surface oxidation. The temperature (650°C) and the time (4 h) were chosen to obtain a NiO film thickness in the 1-μm range (Herchl et al., 1972). The atmosphere was a continuous flow of 1 L/min of oxygen. Rutherford backscattering spectrometry (RBS) analysis performed with a 2-MeV beam of He^+ ions yields a thickness of 0.75 μm for the NiO film overlying the Ni bulk, with an oxygen concentration $C(\mathrm{O}) = 50 \pm 2$ at.%, i.e., almost stoichiometric, in agreement with previous articles by other authors (Herchl et al., 1972; Atkinson, 1985; Egerton & Cheng, 1994). The subsequent step was the removal of a 300-μm-thick slice from the oxidized face by electropolishing, resulting in an NiO/Ni sample more suitable than the original 2-mm-thick standard for the following FIB thinning procedure.

Wedge Thinning of a TEM Lamella by FIB

The lamella was prepared using the FIB lift-out method (Giannuzzi et al., 1997) with an FEI Dual Beam Strata 235M system (FEI Company, Hillsboro, OR, USA). As a first step, a 1.5-μm-thick, 20-μm-long, and 4-μm-deep lamella was sculpted into the bulk, 300-μm-thick sample by milling two opposite rectangular trenches (separated by the lamella) with a high-current FIB. The tip of a nanomanipulator was then brought in touch with the top of the lamella and welded to it by FIB-induced deposition of Pt gas precursor. Once secured to the tip, the lamella was released from the substrate by FIB cuts along the bottom and the sides and lifted-out by the nanomanipulator. Finally, the lamella was attached to a special TEM grid by Pt deposition and released from the tip by FIB cut.

The thinning and wedge shaping of the lamella was performed at this stage. A low-current FIB was repeatedly scanned parallel to the sidewalls, along a line advancing toward the center of the lamella. This procedure, known as lamella polishing, results in sidewalls cleaning from material deposited during the milling and Pt-deposition steps, and in a thinning of the lamella. The wedge shape was obtained by rotating the scan line by 6° with respect to the lamella axis. A lateral and a top view of the wedge-shaped lamella are shown in Figures 1 and 2, respectively. In Figure 3 a projection sketch of the lamella shows that the final sidewalls are not exactly parallel but have a 1.5° slope that replicates the Gaussian-like intensity profile of the FIB beam.

It has been demonstrated that, by properly choosing the milling conditions, no stoichiometry change, detectable by EDS, is introduced into TEM lamellas by FIB preparation (Hutchinson et al., 2003). In our preparation conditions (30-keV Ga^+ ions impinging normal to the surface), the projected range (Rp) of ions into the sidewalls of the NiO wedge is $Rp = 3.7 \pm 2.5$ nm (Holzapfel et al., 2007); therefore, the influence of ion damage on energy dispersive spectrometer (EDS) data is at most 10% in the thinnest point of the wedge (120 nm). The lack of deviation from the fitted curve to our O and Ni concentration data down to the lowest sampled thickness (see Fig. 5) confirms the reliability of the FIB technique as a method for preparing a wedge lamella representative of bulk composition.

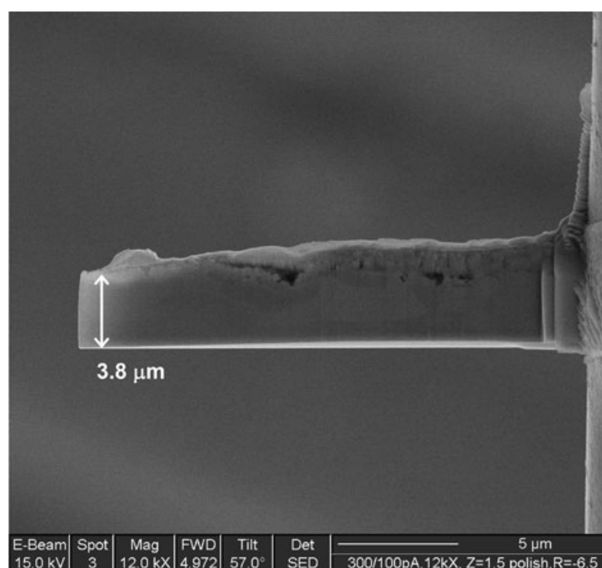

Figure 1. Lateral view of the NiO/Ni lamella. The direction of the STEM beam is perpendicular to the image plane. The local sample thickness increases from left to right.

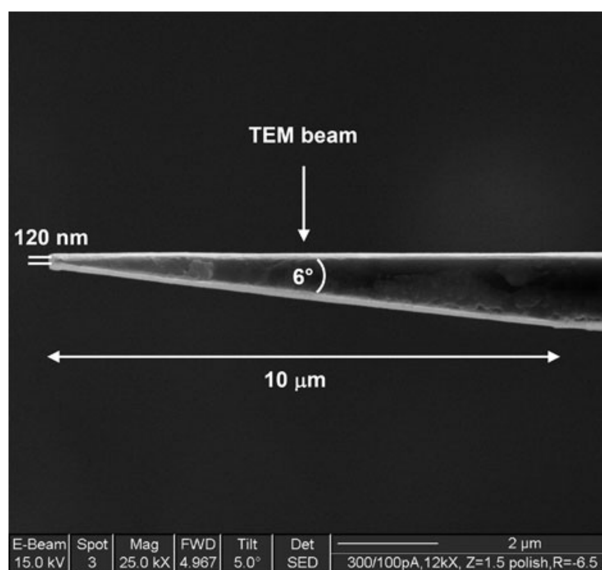

Figure 2. Top view of the lamella, showing the 10-μm-long wedge. The local thickness at the apex of the wedge is ranging from 120 nm to 320 nm at front and back lamella surfaces (see Fig. 1), respectively.

Experimental STEM+EDS Details

For the observations of the wedge-lamella, an FEI Tecnai F20ST STEM (FEI, Hillsboro, OR, USA), operating at 200 kV with a spot size of about 1 nm, was employed. A Gatan 1K×1K slow scan charge-coupled device camera (Gatan, Inc., Pleasanton, CA, USA) has been used for imaging purposes. The X-ray microanalysis work was performed with an EDAX EDS (EDAX, Mahwah, NJ, USA), including a

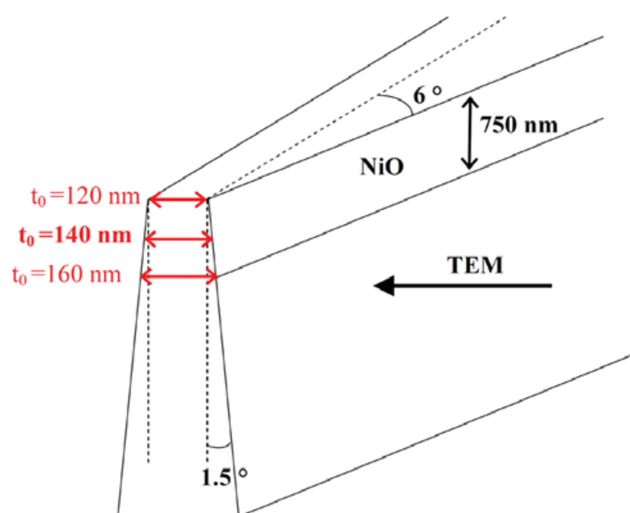

Figure 3. Projection sketch of the lamella shown in Figures 1 and 2. The relevant quotes of the different length, width, and wedge angles are reported, together with the direction of the 200-kV electron beam used for the X-ray microanalytical measurements, performed by the EDS attachment of the Tecnai F20ST STEM.

Si(Li) detector fitted to the microscope. The spectra are acquired as 10-point line scans drawn in the NiO region of the NiO/Ni lamella, which is imaged by using a high-angle annular dark-field (HAADF) detector. To reduce the sample drift during the analysis, the automatic antidrift correction has been activated. The sample was tilted toward the EDS detector by an angle $\alpha = 20°$, which results in a take-off angle $\psi = 37.3°$, according to the relationship $csc\psi = \cos\alpha/\sin(\alpha + e)$ (Zaluzec et al., 1981), where e is the elevation angle of the EDS detector with respect to the horizontal plane ($e = 14.7°$ in the Tecnai F20ST microscope). In the X-ray spectra obtained in each point of a 3,000-nm-long line scan, the OKα and NiKα peak intensities are measured and their relative C(O) and C(Ni) concentrations are evaluated. For quantification the ES Vision software by EmiSpec Systems, Inc. (Tempe, AZ, USA, www.fei.com) has been employed, which is based on the Cliff-Lorimer approach (Cliff & Lorimer, 1975). The results have been compared with both those deduced for the extrapolation method (Van Cappellen, 1990) and those obtained by the Monte Carlo method (Rosa & Armigliato, 1989).

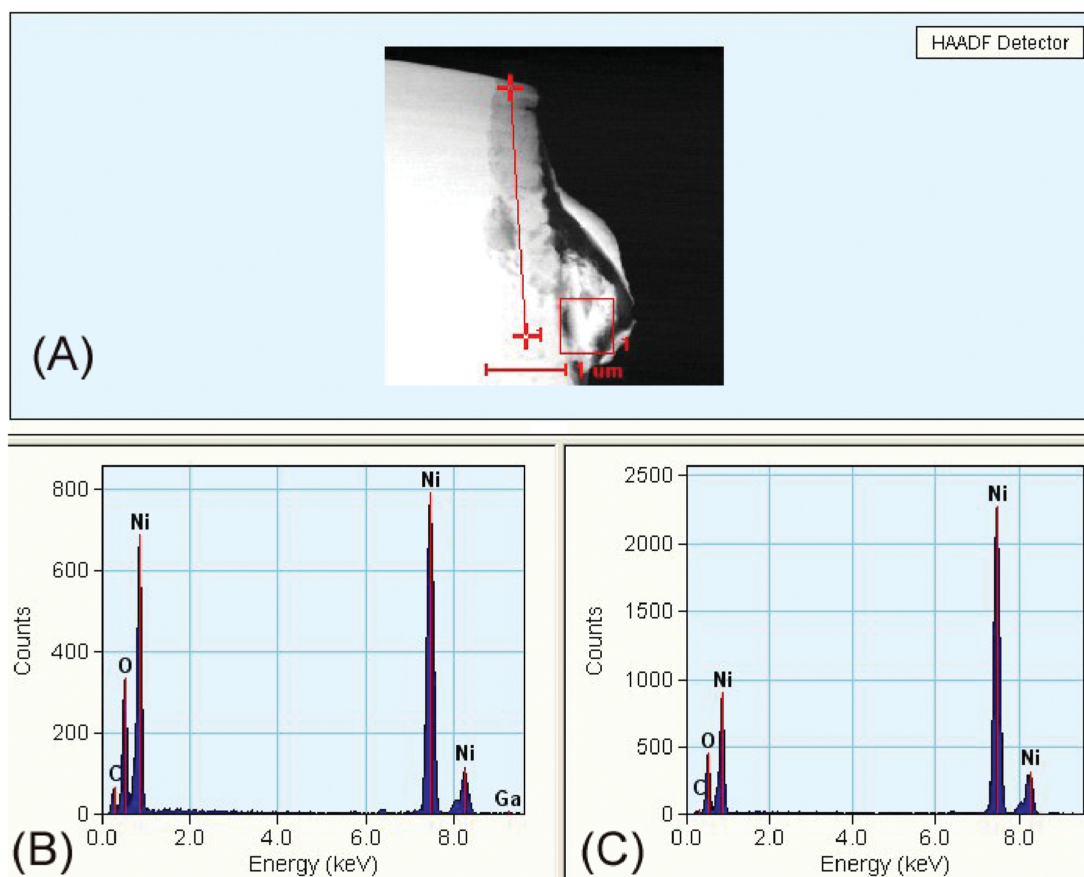

Figure 4. STEM image and EDS spectra taken on a 3,000-nm-long line scan. **a:** The NiO film is almost vertical and clearly distinguishable from the the bulk Ni substrate on its left. The two red crosses correspond to the thinnest (top) and the thickest (marked as 1) analyzed points, respectively. The square box on the right (also marked #1) is used by the software TIA of the Tecnai STEM for the drift correction with the cross-correlation method. **b:** EDS spectrum taken in the thinnest point of the line scan. In addition to the OK and the NiK (and NiL) peaks, a small carbon peak is visible, whereas no GaK peak, related to the FIB ion beam, is detectable. **c:** EDS spectrum taken in the thickest point of the line scan. Note the much higher vertical full scale value with respect to the spectrum on the left. Tilt angle: 20°, take-off angle 37.3°.

Results

In Figure 4a the STEM image taken in the NiO region of the cross section obtained by the FIB thinning of the surface-oxidized bulk Ni standard is reported. The X-ray spectra have been taken in 10 points along the 3-μm line scan shown as a straight line. The crosses at the end points of the line scan correspond to the position where the first and tenth spectrum have been taken, which are reported in Figures 4b and 4c, respectively. The red square box is used for the antidrift correction by the cross-correlation method. The OK and the NiK peaks are those used for quantification purposes. It is worth noting that no GaK peak, due to the Ga beam of the FIB, is visible.

For the determination of the experimental k(O-Ni) Cliff-Lorimer coefficient, in the thin film approximation (no absorption), three different methods have been employed.

Extrapolation Method

According to Van Cappellen (1990), it is based on the following procedure, starting from the integrated peak intensities calculated from the acquired X-ray spectra of the line scan:

1. The 10 spectra are quantified with the Cliff-Lorimer equation, assuming a stoichiometric composition and putting all k-factors equal to 1, under the thin film approximation (no absorption).
2. A plot of C(O) and C(Ni) wt% concentrations versus net NiK X-ray intensity is drawn.
3. The chart is fitted with a linear trendline (more rarely, with a parabolic trendline).
4. The trendline, *extrapolated* to zero thickness, represents a *virtual* concentration.
5. Dividing the *true* concentration ratio by the *virtual* concentration ratio yields the measured k(O-Ni) factor.

In our case, linear extrapolation of OK and NiK intensities to zero yields $C(\mathrm{O}) = 21.6 \pm 0.7$ wt% and $C(\mathrm{Ni}) = 78.4 \pm 0.7$ (*virtual* concentrations, Fig. 5), respectively, wherefrom, as

$$k(\text{O-Ni}) = \frac{[C(\mathrm{O})/C(\mathrm{Ni})]virtual}{[C(\mathrm{O})/C(\mathrm{Ni})]stoichiometric}$$

a value close to 1 is obtained ($k = 0.99$).

It must be noted that this result would not be accurate in the presence of a significant contribution to the primary OK intensity from the secondary fluorescence due to the NiL X-rays. However, the calculation of this effect according to the formulae reported in the literature (Nockolds et al., 1980; Anderson et al., 1995) shows that this contribution is of the order of 10^{-3}, thus quite negligible.

Monte Carlo Calculations

For the reader's convenience we recall briefly the Monte Carlo computer model (see Rosa & Armigliato, 1989 and references therein). The physical model adopts the single-scattering approach, in which the angular deflection is determined by the elastic scattering and the energy loss between

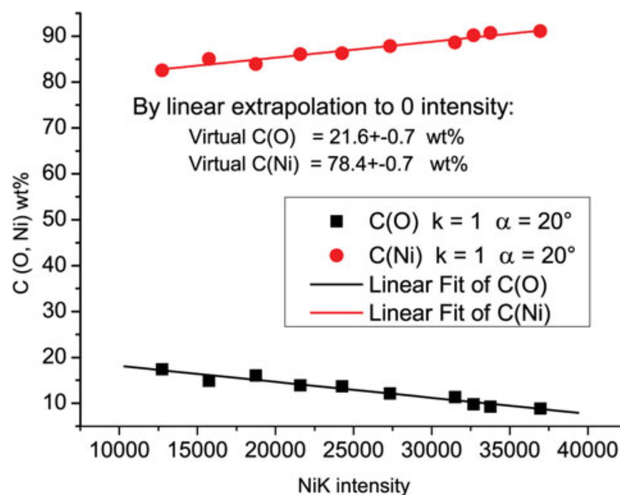

Figure 5. Plot of O and Ni concentrations versus NiK intensity, generated in the different points in the line scan. The curves are fitted with a linear trendline. The extrapolation to zero intensity (thickness) yields *virtual* concentrations, wherefrom the experimental Cliff-Lorimer coefficient k(O-Ni) can be calculated (see text for details).

scattering points is given by the continuous slowing down approximation of the Bethe law. The Wentzel potential is employed to derive the cross section for elastic collisions; the Bethe-Williams ionization cross section is chosen. The relativistic Bethe stopping power has been adopted to describe energy dissipation by electrons in the target. The code can deal with any film thickness in multilayer systems.

With fixed O and Ni concentrations, we computed the $I(\mathrm{OK})/I(\mathrm{NiK})$ ratio as a function of thickness t, from $t \sim 0$, up to 500 nm. The t values chosen for the calculations include those measured from the wedge geometry in Figures 2 and 3 for the probe position in the different points of the line scan, as reported in Table 1.

Figure 6 shows the $I(\mathrm{OK})/I(\mathrm{NiK})$ MC computed intensity ratios versus t with $C(\mathrm{O}) = 21.4$ wt% (= 50 at.%) and the corresponding experimental intensity ratios. The experimental points are fitted with a negative exponential function, according to the thickness dependence of the X-ray absorption correction (Goldstein et al., 1977).

The result is that the MC ratio at $t = 0$ is 0.344, while the exponential fit of the experimental points is at $t = 0$ $I(\mathrm{OK})/I(\mathrm{NiK}) = 0.282$. This ratio (MC) corresponds to a value of k(thin) equal to 0.79. Repeating the MC calculations for $C(\mathrm{O}) = 48$ or 52 at.% results in $t = 0$ $I(\mathrm{OK})/I(\mathrm{NiK}) = 0.317$ and 0.372, respectively. The difference between the two plots (MC and experimental) is in any case quite significant. This is most probably due to the choice of the physical parameters, as well as of the detector efficiency. It is worth noting that, though the Bethe-Williams ionization cross section is maybe inadequate to account for the X-ray generation in the investigated NiO film, the choice of the Powell cross section yields MC intensity ratios even more different from the experimental ones.

It should be also pointed out that computing the k(thin) coefficient from the experimental intensity ratio at $t = 0$, a

Table 1. Local Thickness of the NiO Film for the Different Points of the 3-μm-Long Line Scan in Figure 4.*

10-point Line Scan		Local Thickness t (nm)	
Point #	t	Point #	t
1	140	6	315
2	175	7	350
3	210	8	385
4	245	9	420
5	280	10	455

*The values are measured from the geometry of the wedge-shaped lamella (Figs. 2, 3).

value of 0.97 is obtained; this compares quite favorably with the corresponding one found by using the extrapolation method [k(thin) = 0.99, see previous paragraph and Table 2]. The experimental curves in Figures 5 and 6 are plotted as a function of NiK intensity and local film thickness, respectively; although the extrapolation method by Van Cappellen (1990) is perhaps more accurate, the error associated to the ratio 0.282 ($t = 0$) in Figure 6 is about 3%; therefore, the k(thin) = 0.99 value found from Figure 5 is not really different, being comprised into this error range. In any case, this agreement is in turn a proof of the accuracy of the measurements of the geometrical factors of the lamella (Figs. 2, 3).

k-Factors Embedded into the ESVision Software

The software implemented into the EDAX EDS fitted to the Tecnai microscope (ESVision by Emispec Systems, Inc.) includes k-factor *theoretical* values for any element, calculated according to the Cliff-Lorimer treatment. They are reported in the quantification of the sample composition as wt%, although both atomic and weight concentrations are shown. As in many commercial software packages for X-ray thin film microanalysis, for historical reasons k-factors are expressed relative to silicon, a common element in geological silicates. In our case $k(\text{O}) = k(\text{O})/k(\text{Si}) = 1.962$ and $k(\text{Ni}) = k(\text{Ni})/k(\text{Si}) = 1.511$. This results in a k(O-Ni) factor equal to $[k(\text{O})/k(\text{Si})]/[k(\text{Ni})/k(\text{Si})]$, i.e., 1.30; this value is markedly different from those obtained by the two other methods reported above and summarized in Table 2.

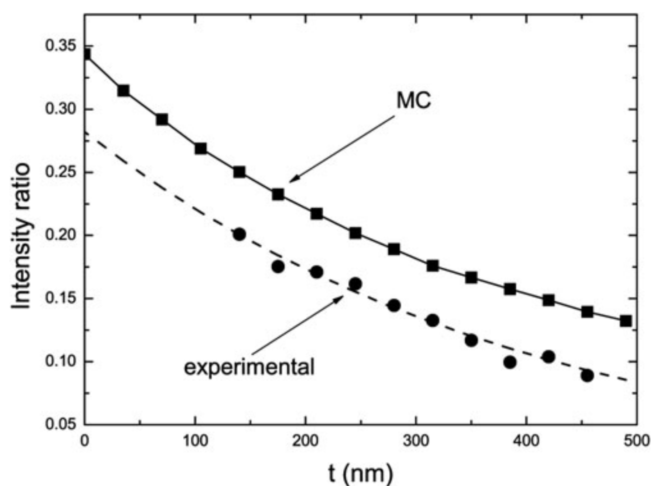

Figure 6. Monte Carlo (MC) and experimental plots of the I(OK)/I(NiK) X-ray intensity ratio as a function of the local thickness in the wedge-shaped NiO lamella. The full circles and most of the full squares correspond to the thickness of the 10 different experimental points of the line scan in Figure 4 (see Table 1).

Table 2. Comparison of the k(O-Ni) Factors Obtained by the Three Methods of Quantification of the X-Ray Spectra Taken in the NiO Film.

Method	Experimental (Extrapolation Method)	Monte Carlo	ESVision Software
$k(\text{O-Ni})^{thin\,a}$	0.99	0.79	1.30

[a] k^{thin} (= k^{gen}) is the value fulfilling the thin film approximation (no absorption). This also corresponds to the (constant) X-ray intensity ratio generated in the different points of the film.

Discussion

The use of the FIB technique to prepare an Ni-O standard suitable for a quantitative X-ray microanalysis based on the extrapolation method presents an advantage with respect to a conventional plan section. The measurement of the local thickness can be directly accurately obtained in each point of the line scan, directly from the geometry of the wedge FIB lamella (Figs. 2, 3), thus avoiding the use of other techniques in the electron microscope. This information allows one to obtain, from the Monte Carlo calculations, accurate values of the absorption correction k(abs)(O-Ni), which must be taken into account to obtain the film composition from the Cliff-Lorimer equation in the points where the thin film approximation cannot be used (this occurs in all 10 points of the above reported experiment). Taking $k(\text{thin}) = 1$, the film composition has been calculated in each of the 10 analyzed points from the ratio $C(\text{O})/C(\text{Ni}) = I(\text{O})/I(\text{Ni})^{*}k(\text{abs})(\text{O-Ni})$. Figure 7 shows that the deviation from the true composition [$C(\text{O})/C(\text{Ni}) = 0.2726$ in weight] is within ±10% in the full thickness range (140–455 nm), which is generally considered as reasonable in thin film X-ray microanalysis by (S)TEM. In addition, it is worthwhile noting that the values of the k(abs) coefficients, deduced from the Monte Carlo calculation, result in good agreement with those obtained from the equation by Goldstein et al. (1977). It is also worth noting that no correlation has been found between the variation of the deviation from the nominal film composition and the variation of the local contrast in the HAADF image (Fig. 4).

Finally, note that the alternative choice of the commercial NiO/C standard, employed in a previous article on quantitative X-ray microanalysis by the Monte Carlo method (Armigliato & Rosa, 2009), is less appropriate for the determination of the experimental thin k(O-Ni) factor than the wedge-thinned lamella described in this work. Indeed, it is recommended instead for evaluating the performance of a

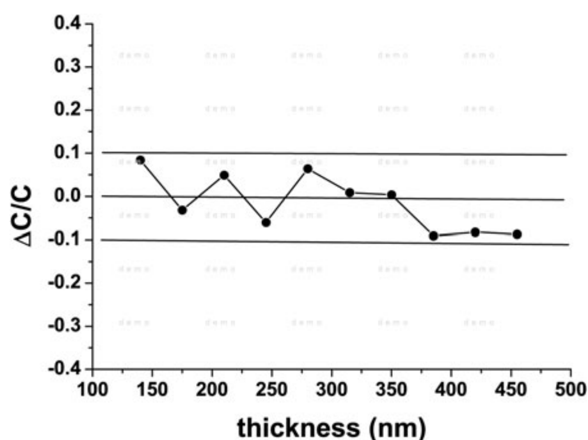

Figure 7. Deviation of the $C(\mathrm{O})/C(\mathrm{Ni})$ ratio ($\Delta C/C$) from the true value (0.2726 in weight) in the points of the line scan in Figure 4. The absorption correction has been calculated by Monte Carlo. A maximum deviation of $\pm 10\%$ (marked by the two horizontal lines) is found in the whole thickness range.

TEM-EDS combination (Egerton & Cheng, 1994) rather than as a standard to obtain the Cliff-Lorimer factors; by the way, the absorption correction of this 55-nm-thick film is not negligible, and the 30-nm C film beneath it is ignored. However, we have determined the OK and NiK X-ray intensities from spectra taken in this film, in the same experimental conditions as in the above-reported experiment on the wedge FIB lamella. The calculation of the Ni-O film composition, performed assuming the absorption correction obtained from Monte Carlo for a thickness of 55 nm, yields a value quite close to the true one [$C(\mathrm{O})/\mathrm{C(Ni)}$ differs from the true value by less than 2%]. This confirms the correctness of the Cliff-Lorimer factor $k(\mathrm{O\text{-}Ni}) = 1$ value obtained in this article.

Conclusions

The method described in this article to obtain a wedge-shaped standard NiO film by FIB preparation allows an accurate determination of the local thickness in the different points of a STEM line scan.

A useful application of this sample is the experimental determination of the Cliff-Lorimer *k*-factor for quantitative X-ray microanalysis. When using the extrapolation method, this procedure of film preparation represents a clear improvement with respect to the usual method based on the uncontrollable slope of a plan section of the sample. It also makes the comparison with the corresponding Monte Carlo calculations more feasible.

In the example reported in this article, the Cliff-Lorimer $k(\mathrm{O\text{-}Ni})$ factors are obtained by three methods (extrapolation, Monte Carlo, and the ESVision software for thin film X-ray microanalysis implemented into the Tecnai F20 STEM). The results clearly demonstrate that the *experimental* coefficients are markedly different from the *theoretical* ones and confirm that their use has to be preferred for an accurate quantification of thin films by X-ray microanalysis.

Acknowledgments

The authors are indebted to I. Elmi and M. Ferri (IMM Institute, thermal treatments), CNR-S3 (FIB), M. Bianconi (IMM Institute, RBS), ISTA s.r.l. (mechanical treatments), and D. Nobili (IMM Institute) for useful discussions.

References

Anderson, I.M., Bentley, J. & Carter, C.B. (1995). The secondary fluorescence correction for X-ray microanalysis in the analytical electron microscope. *J Microsc* **178**, 226–239.

Armigliato, A. & Rosa, R. (2009). X-ray microanalysis combined with Monte Carlo simulation for the analysis of layered thin films: The case of carbon contamination. *Microsc Microanal* **15**, 99–105.

Atkinson, A. (1985). Transport processes during the growth of oxide films at elevated temperature. *Rev Mod Phys* **57**, 437–470.

Cliff, G. & Lorimer, G.W. (1975). The quantitative analysis of thin films. *J Microsc* **103**, 203–207.

Egerton, R.F. & Cheng, S.C. (1994). Characterization of an analytical electron microscope with a NiO test specimen. *Ultramicroscopy* **55**, 43–54.

Giannuzzi, L.A., Drown, J.L., Brown, S.R., Irwin, R.B. & Stevie, F.A. (1997). Focused ion beam milling and micromanipulation lift-out for site specific cross-section TEM specimen preparation. *Mat Res Soc Proc* **480**, 19.

Goldstein, J.I., Costley, J.L., Lorimer, G.W. & Reed, R.J.B. (1977). Quantitative X-ray analysis in the electron microscope. In *Scanning Electron Microscopy 1977*, Johari, O. (Ed.), Vol. 1, pp. 315–324. Chicago, IL: IITRI.

Herchl, R., Kooi, N.N., Homma, T. & Smeltzer, W.W. (1972). Short-circuit diffusion in the growth of nickel oxide scales on nickel crystal faces. *Oxid Met* **4**, 35–49.

Holzapfel, C., Soldera, F., Faundez, E.A. & Mücklich, F. (2007). Site-specific structural investigations of oxidized nickel samples modified by plasma erosion processes. *J Microsc* **227**, 42–50.

Hutchinson, C.R., Hackenberg, R.E. & Shiflet, G.J. (2003). A comparison of EDS microanalysis in FIB-prepared and electropolished TEM thin foils. *Ultramicroscopy* **94**, 37–48.

Nockolds, C.E., Nasir, M.J., Cliff, G. & Lorimer, G.W. (1980). X-ray fluorescence correction in thin foil analysis and direct methods for foil thickness measurement. *Electron Microscopy and Analysis 1979: Proc. EMAG 79*, University of Sussex, Brighton, 1979, Mulvey, T. (Ed.), Inst. Physics Conf. Series 52, pp. 417–420. Bristol, UK: Institute of Physics.

Rosa, R. & Armigliato, A. (1989). Monte Carlo simulation of thin-film X-ray microanalysis at high energies. *X-Ray Spectrom* **18**, 19–23.

Van Cappellen, E. (1990). The parameterless correction method in X-ray microanalysis. *Microsc Microstruct Microanal* **1**, 1–22.

Westwood, A.D., Michael, J.R. & Notis, M.R. (1992). Experimental determination of light-element *k*-factors using the extrapolation technique: Oxygen segregation in aluminium nitride. *J Microsc* **167**, 287–302.

Williams, D.B. & Carter, C.B. (2009). Quantitative X-ray analysis. In *Transmission Electron Microscopy*, 2nd ed., part 4, chap. 35. New York: Springer.

Zaluzec, N.J., Maher, D.M. & Mochel, P.E. (1981). Effect of detector geometry on AEM-based X-ray microanalysis: I. Theoretical. In *Analytical Electron Microscopy-1981*, Geiss, R.H. (Ed.), pp. 25–28. San Francisco, CA: San Francisco Press.